EUROPEAN JOURNAL OF BIOMEDICAL AND PHARMACEUTICAL SCIENCES
http://www.ejbps.com

ISSN 2349-8870
Volume: 5
Issue: 3
532-537
Year: 2018

ANTICANCER EFFICACY OF GELATINE-ETOPOSIDE NANOPARTICLES IN NCI-H460 CELL LINE

Lakhya Jyoti Gogoi[1*] and Kamala Kanta Borah[2]

[1]Department of Medical Lab and Molecular Diagnostic Technology, Mangaldai College, Mangaldai.
[2]Department of Chemistry, Mangaldai College, Mangaldai, Assam.

***Corresponding Author: Lakhya Jyoti Gogoi**
Department of Medical Lab and Molecular Diagnostic Technology, Mangaldai College, Mangaldai.

Article Received on 08/01/2018 **Article Revised on 29/01/2018** **Article Accepted on 18/02/2018**

ABSTRACT
Chemotherapy has been a major treatment methodology for malignant tumors. Etoposide (ETP), as one of the oldest and best antieoplastic chemotherapy drugs. However, ETP has some drawbacks such as unstabilization, poor water solubility and short biological half time, which limit the uses of ETP in medicine. The aim of the present study was to encapsulate ETP in gelatin nanoparticles (GNPs) and to study its anticancer efficacy in NCI-H460 non small cell lung carcinoma cell line. SEM and DLS studies have revealed that the prepared ETP-GNPs possess spherical shape with a mean diameter of 186 nm. Through the Schiff base reaction and hydrogen bond interaction of cross-linker glutaraldehyde has been achieved the successful encapsulation of ETP in GNPs. In vitro drug release kinetics indicated that there was an initial burst release followed by a slow and sustained release of ETP from GNPs. Further, ETP-GNPs exhibits increased intracellular ROS levels and apoptotic morphological changes in NCI-H460 cells when compared to bulk ETP treatment alone. Hence, GNPs carrier system might be a promising mode for controlled delivery and for improved therapeutic index of poorly water soluble ETP.

KEYWORDS: *Chemotherapy, Nanoparticle, Anticancer, Etoposide (ETP), Gelatin Nanoparticles (GNPs).*

INTRODUCTION
Cancer, the second major cause of human death, spares neither men nor women. Cancer develops when normal cells in a part of the body begins to grow out of control. The development of cancer is multifunctional process that usually takes several decades[1]; it causes a major public health problem worldwide. It was once considered an incurable disease, but today most patients diagnosed with early stage cancer will survive their illness.[2]

Lung cancer is the second most commonly diagnosed cancer in both man and women and the leading cause of cancer deaths. More people die from lung cancer than breast, colon and prostate cancers combined. Non-small cell lung cancer (NSCLC), that constitutes 75-80% of all lung cancer, is one of the most frequent tumors in the elderly.[3] Chemotherapy is an important and often necessary form of anticancer therapy because it is able to reduce the risk of recurrence after surgery. Chemotherapy, being a major treatment modality used for the control of advanced stages of malignancies and as a prophylactic against possible metastasis, exhibits severe toxicity on normal tissues.[4][5]

Etoposide (ETP) is a most commonly used as a chemotherapy drug for cancer treatment (Cristina et al., 2002) and chemically designated as 40-emethylepipodophyllotoxin- 9-(4,6-O-ethylidene)-b-D-glucopyranoside, is an important antineoplastic agent currently in clinical use for the treatment of small cell lung cancer, testicular cancer and lymphomas.[6][7] Its mechanism of action involves breakage of DNA strands by reversible interaction with topoisomerase II.[8] Low and erratic oral absorption of ETP has been attributed to drug precipitation in the gastrointestinal lumen due to poor aqueous solubility, pH related degradation and efflux by p-glycoprotein transporter. ETP is poorly soluble in water has anti-neoplasic activity particularly against various types of solid tumors. Nanoparticles are biodegradable polymers, featured by their small size, acceptable biocompatibility high drug encapsulation efficiency especially for hydrophobic drugs, controlled drug release, high cellular internalization, desired pharmacokinetics and long circulation half-life. Nanoparticles drug delivery systems will also reduce the drug dosage frequency and will increase the patient compliance.

2. MATERIAL AND METHODS
2.1. Chemicals
Etoposide (ETP), Gelatin, thiobarbituric acid (TBA), phenazine methosulphate (PMS), nitroblue tetrazolium

(NBT), 5, 5-dithiobis 2-nitrobenzoic acid (DTNB), 3-(4, 5-dimethyl-2-thiaozolyl)-2, 5-diphenyl- tetrazolium bromide (MTT), 2-7-diacetyl dichlorofluorescein (DCFH-DH), Rhodamine 123 (Rh 123), ethidium bromide, acridine orange, cell culture chemicals such as heat inactivated fetal calf serum (FBS), minimum essential medium (MEM), glutamine, penicillin-streptomycin, EDTA, trypsin, low melting agarose, normal melting agarose, phosphate buffered saline (PBS) and reduced glutathione (GSH) were purchased from Sigma chemical Co., St. Louis, USA.

2.2. Preparation and characterization of ETP-GNPs

2.2.1. Preparation of etoposide loaded GNPs

Gelatin nanoparticles were prepared by coacervation-phase separation technique with slight modifications.[9] Briefly, 200 mg of gelatin-B was dissolved in distilled water (20 mL) under constant heating at 40 ± 1 °C. ETP (10 mg dissolved in 500 µL of DMSO) was added in aqueous polymer phase, followed by drop wise addition of span 80 (30 mL) to form GNPs. At the end of the process, glutaraldehyde solution (25% v/v aqueous solution) was added as a cross-linking agent, and the solution was stirred for 12 h at 700 rpm (Remi, Mumbai, India). DMSO was removed with repeated mild washing with distilled water. The ETP-GNPs were stored as freeze-dried powder under vacuum (2 mm Hg) at 25 °C for further investigations.

2.2.2. Particle size, size distribution and zeta potential

DLS (Zetasizer Nano, Malvern Instruments Ltd. United Kingdom) was used to measure the average size and size distribution of the prepared nanoparticles. Three different batches were analyzed to give an average value and standard deviation for the particle diameter and zeta potential.

2.2.3. Scanning electron microscopy (SEM)

The morphological features of ETP-GNPs were examined by scanning electron microscopy (Quanta 200F, FEI, Hillsboro, OR, USA). The samples were sprinkled onto a double-sided tape and sputter-coated with a 5 nm thick gold layer. The inner structures of nanoparticles were observed after fracturing nanoparticles by a razor blade.

2.2.4. Fourier transform-infrared spectroscopy (FT-IR)

FT-IR spectra were recorded by using a Spectrophotometer (Perkin Elmer 1700 FT-IR spectrometer, USA). Gelatin and ETP-GNPs samples were prepared by processing compressed KBr disks.

2.2.5. In vitro drug release studies

The in vitro drug release tests were carried out on ETP and ETP-GNPs formulation. Fifty milligrams of each sample was suspended in 100 mL of PBS buffer (various pH ranges) at 37 ºC and placed in an incubator shaker at 1200 rpm. At predetermined time intervals, 3 ml of aliquots was withdrawn and the concentration of drug released was monitored by UV spectrophotometer (Elico SL159, India) at 270 nm. The dissolution medium was replaced with fresh buffer to maintain the total volume. The drug release percent was determined by following equation (1):

$$\text{Drug release (\%)} = \frac{C_{(t)}}{C_{(0)}} \times 100$$

Where $C_{(0)}$ and $C_{(t)}$ represents the amount of drug loaded and amount of drug released at a time t, respectively. All studies were done in triplicate.

2.3. Anticancer efficacy of ETP-GNPs

2.3.1. Cell culture

The present work was carried out in human lung cancer cell line (NCI-H460). This cell line was obtained from National Centre for Cell Science (NCCS), Pune, India. The NCI-H460 cells were cultured as monolayer in RPMI-1640 medium, supplemented with 10% fetal bovine serum (FBS), 1% glutamine, and penicillin-streptomycin at 37°C in 5% CO_2 atmosphere. Stocks were maintained in 25 cm^2 tissue culture flasks and used for experiments when in exponential growth phase. Cells were treated with different concentration of ETP and ETP-GNPs (10, 20, 30, 40, 50 and 60 µg/mL) and cytotoxicity was observed after 24 h incubation by MTT assay [10]. IC50 values were calculated and the optimum dose was used for further study.

The NCI-H460 cells were divided into three experimental groups. Group 1: untreated control cells, Group 2: ETP alone (20 µg/mL) treated cells, Group 3: ETP-GNPs (5 µg/mL) treated cells.

2.3.2. Determination of intracellular ROS levels

Intracellular ROS level was measured by using a non-fluorescent probe, 2, 7,-diacetyl dichlorofluorescein diacetate (DCFH-DA) that can penetrate into the intracellular matrix of cells where it is oxidized by ROS to fluorescent dichloro fluorescein (DCF) (Fig: 6 A-B) ETP-GNPs and free ETP treated NCI-H460 cells were seeded in 6 well plates (2 x 106 cells/well) and incubate with 10 µl DCFH-DA (10 µM) at 37 °C for 30 min. Fluorescence measurements were made with excitation and emission filters set at 485 ± 10 nm and 530 ± 12.5 nm respectively (Shimadzu RF-5310 PC spectroflurometer). The cells were also observed under flouresence microscope using blue filter (450-490nm) (Nikon Eclipse TS100, Japan).

2.3.3. Changes in mitochondrial transmembrane potential

The change in mitochondrial membrane potential during ETP-GNPs and ETP treatment condition were analyzed using Rh-123 staining. ETP and ETP-GNPs treated cells were mixed with 1 µL of Rh -123 (5 mmol/L) and kept incubation for 15 min (fig: 8 A-B) Then, the cells were washed with PBS and observed under fluorescence microscope using blue filter (450-490 nm). The fluorescence intensity in treated cells were also recorded using spectroflurometric with excitation and emission

filters set at 485 ± 10 nm and 530 ± 12.5 nm respectively.

2.3.4. Apoptotic morphological changes

Apoptotic nuclei exhibiting typical changes such as nuclear condensation and segmentation were stained by acridine orange (AO) and ethidium bromide EBr) [11]. The control, ETP and ETP-GNPs treated cancer cells were seeded in 6-well plate (3 x 10^4 /well) and incubated in CO_2 incubator for 24 h. The cells were fixed in methanol: glacial acetic acid (3:1) for 30 min at room temperature. The cells were washed in PBS, and stained with 1:1 ratio of AO/EBr. Stained cells were immediately washed again with PBS and viewed under a fluorescence microscope with a magnification of 40x. The number of cells showing features of apoptosis was counted as a function of the total number of cells present in the field.

2.5. Statistical analysis

All quantitative measurements were expressed as means ± SD for ETP, ETP-GNPs and untreated cells. The data were analyzed using one way analysis of variance (ANOVA) on SPSS/PC (statistical package for social sciences, personal computer) and the group means were compared by Duncan's Multiple Range Test (DMRT). The results were considered statistically significant if the P value is less than 0.05.

3. RESULTS

3.1 Particle size, distribution, zeta potential and FT-IR spectrum

DLS results revealed that the average size of the ETP-GNPs was 186 nm and the pdi was found to be 1.000. The surface morphology of the nanoparticles was studied using SEM (Fig: 2) illustrates the SEM image of ETP-GNPs which shows that the nanoparticles were spherical in shape. The major characteristic peaks of ETP (1200-1700 cm-1) and -OH phenolic bending (1200-1600 cm-1) are present in free and GNPs encapsulated ETP (Fig: 3) These ETP peaks have not been present in GNPs alone. Further, GNPs characteristic peaks like –C=O stretching (1634.4 cm-1) and C=H stretching (2856.4 cm-1) are present in the ETP-GNPs.

3.2. In vitro drug release

The average cumulative percentage release profile of ETP from the GNPs at prefixed time intervals was shown in (Fig: 4). Drug release kinetics studies showed that there was an initial burst release of ETP from GNPs up to 48 h and followed by a slow release of ETP from GNPs. ETP-GNPs released 46.6% of ETP at pH 7.4 upon 24 h incubation. After 48 h incubation 75.4% ETP has been released at pH 7.4.

3.4. Anticancer efficacy of ETP-GNPs

3.4.1. In vitro cytotoxicity assay

In vitro percentage cytotoxicity of ETP-GNPs (10, 20, 30, 40, 50 and 60 µg/mL) in NCI-H460 cells shows in (Fig: 5) ETP-GNPs treatment (24 h) showed cytotoxicity on NCI-H460 cells in a concentration dependent manner. There was a 100% cell death at 60 µg/mL concentration of ETP. Conversely, ETP-GNPs showed 100% cell death at 40 µg/mL concentration in NCI-H460 cells. Hence, the inhibitory concentration 50 (IC_{50}) was fixed as 30 µg/mL for ETP and 20 µg/mL for ETP-GNPs in NCI-H460 cells. These optimum doses of ETP and ETP-GNPs were used for the anticancer experiments in NCI-H460 cells.

3.4.2. ETP-GNPs increased ROS generation in NCI-H460 cells

Fluorescence microscopic images show weak ROS generation in the control NCI-H460 cells (Fig: 6 A). Significant ROS production was found in ETP treated cells and a further enhanced ROS generation were found during ETP-GNPs treatment. (Fig: 6 B). shows the spectrofluorometric readings of DCF fluorescence in ETP and ETP-GNPs treated cells. ETP-GNPs showed maximum generation of ROS in NCI-H460 cells when compared with ETP treatment alone.

3.4.3. ETP-GNPs modulates mitochondrial membrane potential in NCI-H460 cells

Mitochondrial membrane potential has been found to be reduced in the ETP-GNPs treated cells when compared with ETP alone treated cells (Fig: 8 A). Fluorescence microscopic images (Fig: 8 B) showed accumulation of Rh-123 dye in the control group. No Rh-123 accumulation was found in ETP-GNPs treated cells as the membrane potential decreased.

3.4.4. Effect of ETP-GNPs on apoptotic morphological changes

Apoptotic morphological changes in different treatment groups are depicted in (Fig: 7 A). Apoptotic features with condensed or fragmented chromatin, indicative of apoptosis, were observed in ETP and ETP-GNPs treated NCI-H460 cells. Control cells showed evenly distributed acridine orange stain (green fluorescence) with no morphological changes whereas ETP and ETP-GNPs treated cells showed apoptotic morphological features and showed ethidium bromide fluorescence due to membrane damage (Fig: 7 B) shows the quantitative result of apoptosis in the different treatment groups. ETP-GNPs treatment showed 90% of apoptotic cells whereas free ETP treatment showed only 60% apoptotic cells.

TABLES AND FIGURES

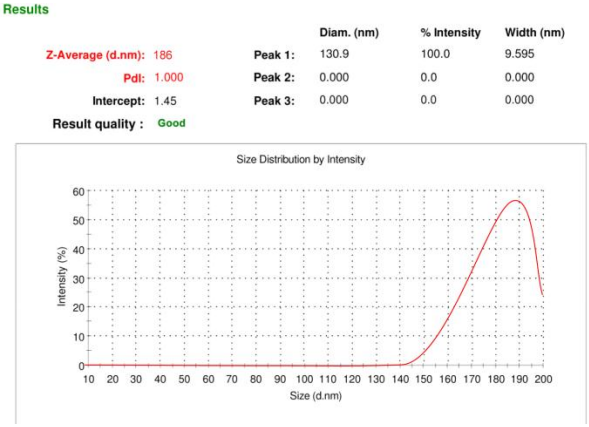

Fig: 1 Particles size distribution of the ETP-GNPs by DLS

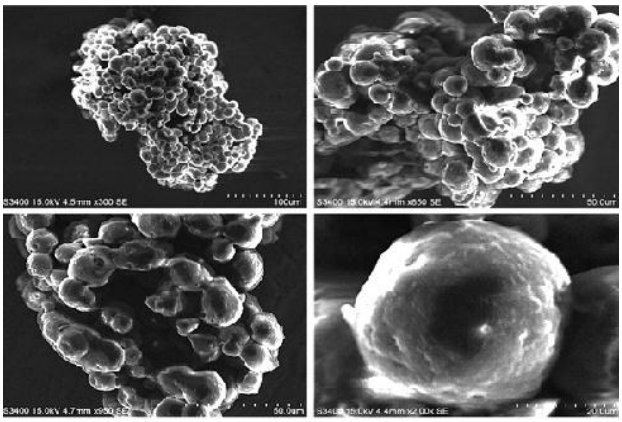

Fig: 2 Morphology of ETP-GNPs by SEM

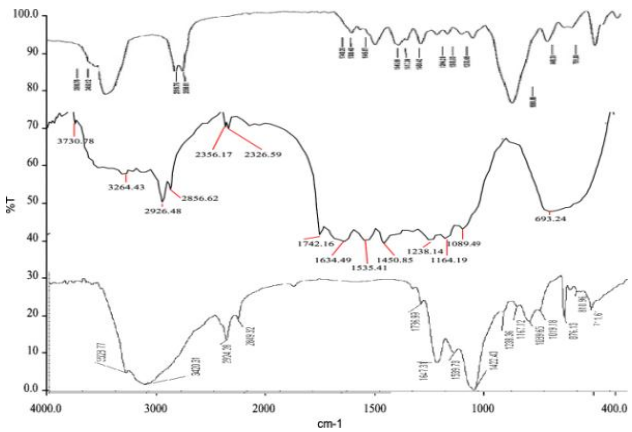

Fig: 3 FT-IR spectrum of (i) ETP (ii) Gelatin and (iii) ETP -GNPs

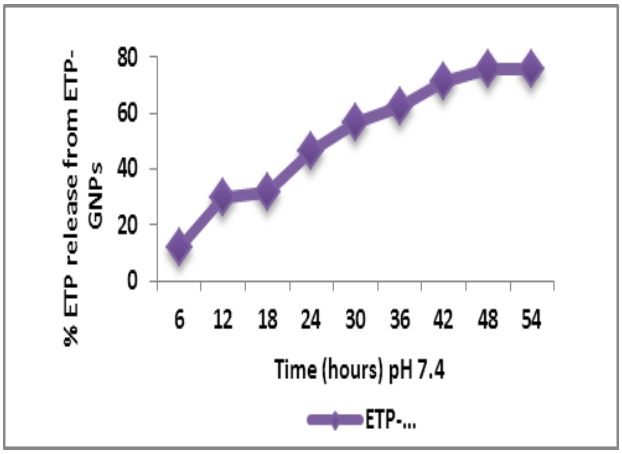

Fig: 4 *In vitro* ETP release kinetics from GNPs at 7.4 pH levels in PBS

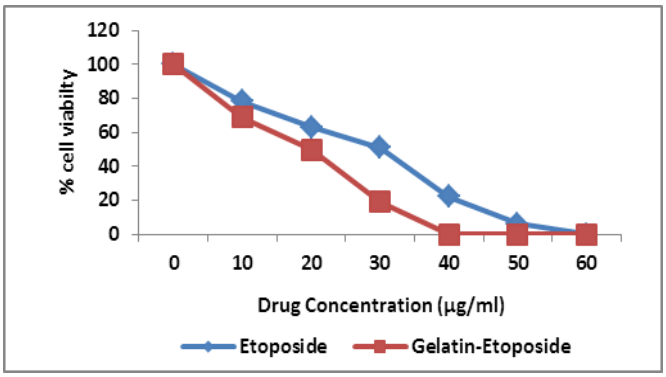

Fig: 5 Effect of ETP and ETP-GNPs on NCI-H460 cell viability (24 h).

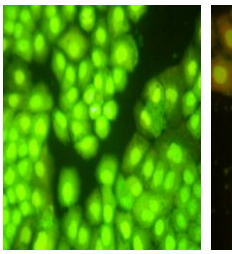

Fig: 6A- Microscopic images show the intracellular ROS levels in NCI-H460 cells

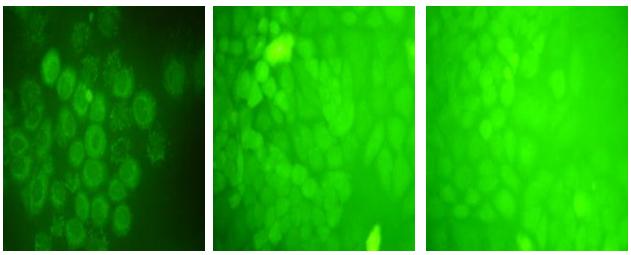

Fig: 7A-Microscopic images show apoptotic morphological changes by EtBr and AO staining.

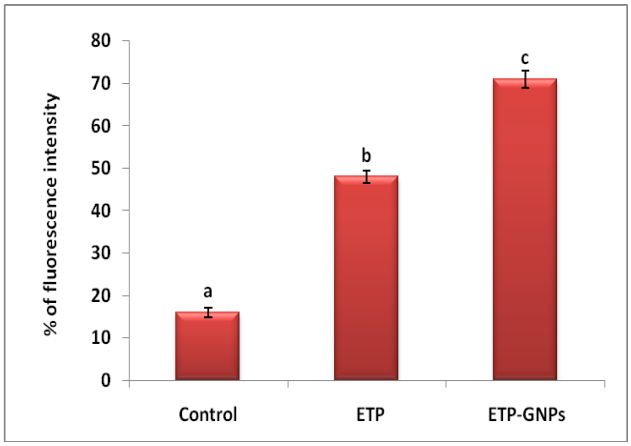

Fig: 6B - Effect of ETP and ETP-GNPs on ROS levels. DCF fluorescence intensity was recorded using spectrofluorometer.

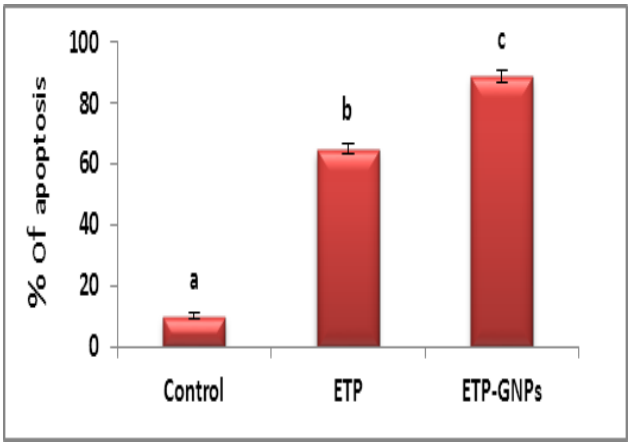

Fig: 7B - Effect of ETP and ETP-GNPs on apoptosis (%) in NCI-H460 cells.

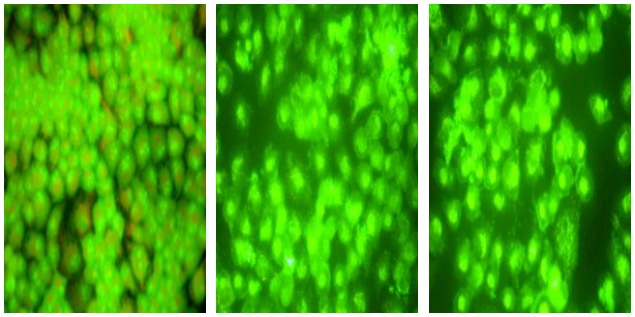

Fig: 8A- Microscopic images show the MMP in NCI-H460 cells.

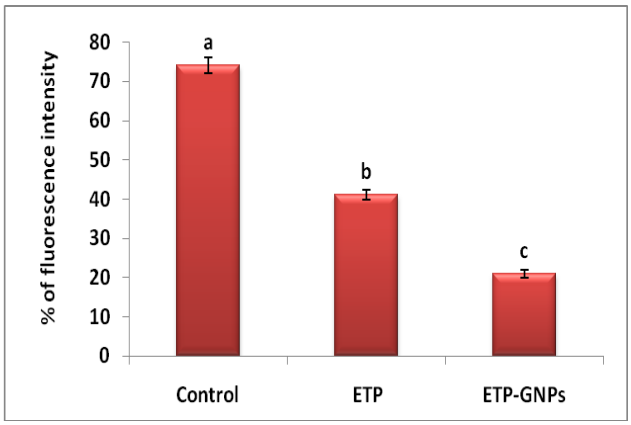

Fig: 8B - Effect of ETP and ETP-GNPs on MMP levels. DCF fluorescence intensity was recorded using spectrofluorometer.

4. DISCUSSION AND CONCLUSION

Etoposide (ETP), chemically designated as 40-emethylepipodophyllotoxin-9-(4, 6-O-ethylidene)-b-D-glucopyranoside, is an important antineoplastic agent currently in clinical use for the treatment of small cell lung cancer, testicular cancer and lymphomas. Its mechanism of action involves breakage of DNA strands by reversible interaction with topoisomerase II. Low and erratic oral absorption of ETP has been attributed to drug precipitation in the gastrointestinal lumen due to poor aqueous solubility, pH-related degradation and efflux by p-glycoprotein transporter.

In this study, we encapsulated ETP into GNPs and investigate its anticancer effect in NCI-H460 cells. The coacervation is recommended for the incorporation of hydrophobic drug into polymeric nanoparticles. In this study, we prepared ETP-GNPs by coacervation-phase separation.

The prepared particles had average size of 186 nm and polydispersity index (PI) of 1.000. As mentioned above, these findings were confirmed by the SEM data which also showed that nanospheres were spherical.

The SEM photomicrographs of the ETP-GNPs showed the prepared ETP-GNPs had smooth surface but with some irregular small particles (Fig: 2), which were attributed to the results of the mechanical stress during the stirring process or the movement of the moisture during the drying period.

Further we evaluated the anticancer activity of ETP-GNPs in NCI-H460 cell line. ETP-GNPs treatment (24 h incubation) significantly decreases % cell viability in NCI-H460 cells. This suggested that an ETP-GNPs treatment was able to inhibit the growth of cancer cells during incubation. The reason for increased cytotoxicity observed in the ETP-GNPs group might be because of the increased cellular uptake. The IC_{50} of ETP-GNPs was slightly lower than that of the ETP alone. This result indicates that the nanoparticles were able to transport more ETP into the cells, thus achieving greater cytotoxicity.

We have observed an increase in intracellular ROS levels as evidenced by increased DCF fluorescence. In the present study, the ETP-GNPs induced metabolic oxidative stress and bioavailability and might be the

reason for increased intracellular ROS production in ETP-GNPs treated NCI-H460 cells. Hence, GNPs enables more accumulation ETP inside the cells and consequently generates more intracellular ROS which might be the reason for enhanced cytotoxicity.

In mitochondrial membrane potential in ETP-GNPs treated and control cells. Mitochondrial membrane potential has been altered during ETP-GNPs treated cells. ETP-GNPs treated cells showed no uptake of Rh 123. This indicates that the mitochondrial membrane potential has been altered during ETP-GNPs treatment. This shows that the mitochondrial membrane potential play a role in ETP-GNPs induced cell death.

The inhibition of cell proliferation and increased ROS level was associated with profound induction of cell apoptosis. To explore the method of the cell death in lung cancer cells by ETP-GNPs we observed apoptotic morphology by AO/EtBr staining. The increased apoptotic incidence during ETP-GNPs treatments clearly indicates the direct and controlled release of ETP intracellularly by GNPs. It might also be due to the better uptake of nanoparticulate ETP which resulted in greater accumulation of delivered ETP inside cancer cell accompany by its sustained release, exerting more percentage of cells in apoptotic phase.

In conclusion, the ETP-GNPs were prepared by a modified coacervation method. SEM and DLS studies have revealed that the prepared ETP-GNPs possess spherical shape with a mean diameter of 186 nm. The successful encapsulation of ETP-GNPs has been achieved. *In vitro* drug release kinetics indicated that there was an initial burst release followed by a slow and sustained release of ETP from GNPs. Further, ETP-GNPs showed enhanced anticancer activity than free ETP by decreasing cell viability and increasing cytotoxicity, intracellular ROS levels and apoptosis in NCI-H460 cells. Based on these results, it can be concluded that the GNPs is an ideal way to deliver ETP because of its high loading efficiency and superior efficacy in cancer cell line and animal model.

ACKNOWLEDGEMENT

Authors are thankful to DBT, Govt. of India for providing necessary funding and the Principal, Mangaldai College for providing the adequate laboratory facilities to complete this work.

REFERENCE

1. Loeb KR, Anerson JP. Multiple mutations and cancer proceedings of the National academy of sciences, 2003; 100: 776-781.
2. Borek C. Antioxydanta and cancer. Science and Medicine. 1997; 4:51-62. Biennial Report 1988-1989. Indian council of Medical Research, 1992, New Delhi.
3. Brown JD, Eraut D, Trask C, et al. Age and the treatment of lung cancer. Thorax, 1996; 51: 564-568.
4. Somkumar AP. Studies on anticancer effects of Ocimum sanc-tum and Withania somnifera on experimentally induced cancer in mice. PhD thesis, J.N.K.V.V. Jabalpur, 2003.
5. Pandey, Govind and Madhuri S. Medicinal plants: better remedy for neoplasm. Indian Drugs. 2006; 43: 869-874.
6. Toffoli, G., Corona, B., Basso, B., Boiocchi, M., Pharmacokinetic optimisation of treatment with oral etoposide. Clin. Pharmacokinet, 2004; 43: 441–466.
7. Sissolak, G., Sissolak, D., Jacobs, P., Human immunodeficiency and Hodgkin lymphoma. Transfus. Apher. Sci., 2010; 42: 131–139.
8. Hande, K.R., Topoisomerase II inhibitors. Update Cancer Ther., 2008; 3: 13–26.
9. Oppenheim RC, Stewart NF. The manufacture and tumor cell uptake of nanoparticles labeled with fluoroscein isothiocyanate. Drug Dev Ind Pharm., 1979; 5: 583–591.
10. Mosmann T. Rapid colorimetric assay for cellular growth and survival: application to proliferation and cytotoxicity assays. J Immunol Methods, 1983; 65(1-2): 55-63.
11. Lakshmi S, Dhanaya GS, Beena Joy, Padmaja G, Remani P. Inhibitory effect of an extract of Curcuma zedoariae on human cervical carcinoma cells. Med chem. Res., 2008; 17: 335-344.